AIP | Journal of Applied Physics

Multifunctional tunable ultra-broadband visible and near-infrared luminescence from bismuth-doped germanate glasses

Beibei Xu, Shifeng Zhou, Dezhi Tan, Zhanglian Hong, Jianhua Hao et al.

Citation: J. Appl. Phys. **113**, 083503 (2013); doi: 10.1063/1.4791698
View online: http://dx.doi.org/10.1063/1.4791698
View Table of Contents: http://jap.aip.org/resource/1/JAPIAU/v113/i8
Published by the AIP Publishing LLC.

JOURNAL OF APPLIED PHYSICS **113**, 083503 (2013)

Multifunctional tunable ultra-broadband visible and near-infrared luminescence from bismuth-doped germanate glasses

Beibei Xu,[1,2] Shifeng Zhou,[1,3] Dezhi Tan,[1] Zhanglian Hong,[1] Jianhua Hao,[2] and Jianrong Qiu[1,4,a)]

[1]*State Key Laboratory of Silicon Materials and Department of Materials Science and Engineering, Zhejiang University, Hangzhou, Zhejiang 310027, People's Republic of China*
[2]*Department of Applied Physics, The Hong Kong Polytechnic University, Hung Hom, Hong Kong*
[3]*State Key Laboratory of Modern Optical Instrumentation, Zhejiang University, Hangzhou 310027, People's Republic of China*
[4]*State Key Laboratory of Luminescence Physics and Chemistry, and Institute of Optical Communication Materials, South China University of Technology, Guangzhou, Guangdong 510640, People's Republic of China*

(Received 15 November 2012; accepted 23 January 2013; published online 22 February 2013)

Here, we present three facile approaches to achieve wavelength tunable luminescence in the same host material with single dopant, i.e., by modulating doping level, preparation temperature, and atmosphere. Based on these methods, ultra-broadband tunable near-infrared luminescence with the largest full width at half maximum of about 500 nm covering the whole windows of optical communication has been obtained in bismuth-doped germanate glasses. Wavelength tunable luminescence is also observed with the change of excitation wavelength. Systematical strategy was followed to approach the physical origin of the near-infrared luminescence and we proposed that three different bismuth active centers contribute to the near-infrared luminescence in the germanate glasses. A comprehensive explanation for the tunable luminescence is given, combining the concentration, energy transfer, and chemical equilibrium of these active centers in the glasses. With the increase of melting temperatures and the increase of reducing extent of the preparation atmosphere, bismuth species transform from Bi^{3+} to Bi^{2+}, Bi^{+}, Bi^{0} and bismuth clusters, and then to bismuth colloid. Of particular interest is that red tunable luminescence was also observed by modulating doping level, preparation atmosphere, and excitation wavelength. Besides, the trapped-electron centers in germanate glasses can interact with bismuth species of high valence states leading to the formation of bismuth active centers of low valence states and the decrease of trapped-electron centers. This tunable ultra-broadband luminescence is helpful for a better understanding of the origin of the near-infrared luminescence in Bi-doped glasses and may have potential applications in varieties of optical devices. © *2013 American Institute of Physics*. [http://dx.doi.org/10.1063/1.4791698]

I. INTRODUCTION

Ever-increasing demand in optical communication, energy, and lighting has raised expanding needs for multifunctional luminescence materials, such as optical fiber materials, photovoltaic energy conversion materials, and lighting materials.[1] However, these stringent requirements are not well met at present, and many challenges are ahead. Specifically, the rapid development of optical communication networks needs for optical fiber data transmission with super high speed and super large capacity. These demands have stimulated interest in optical integrated components such as fiber amplifiers, which are the most essential element of modern optical fiber communication systems.[2] Currently, the high bit rate communication systems use a narrow spectral region of 1530-1610 nm for transmission based on Er-doped fiber amplifiers (EDFA).[2] But narrow gain bandwidth is still a major problem due to the intrinsic narrow *f-f* transitions among the 4*f* orbits of rare-earth ions confined in the inner-shell, which are relatively independent of the host matrix. Moreover, no efficient rare-earth doped fiber lasers exist in the 1150-1500 nm spectral region which could be used in advanced optical communication systems, medicine, astrophysics, and other important applications.[2] Thus, ultra-broadband near-infrared (NIR) luminescence materials are significant for the creation of optical amplifiers and fiber lasers. Besides fiber communication, photovoltaic energy conversion also attracts much attention due to its increasing role in renewable energy and agricultural production.[1,3,4] So far, the most widely used solar cells are based on crystalline silicon, suffering from high production cost and low conversion efficiency.[5] By now, many methods have been used to rise the conversion efficiency of solar cells,[4–9] among them down conversion especially quantum cutting has attracted much attention. Because quantum cutting materials doped with rare earth ions can absorb one high energy photon which cannot be absorbed by solar cells efficiently and transfer it to two or more low energy photons that can be absorbed efficiently by solar cells.[10] However, the absorption

a)Author to whom correspondence should be addressed. Electronic mail: qjr@zju.edu.cn.

arising from the parity-forbidden 4f-4f transitions of rare-earth ions is weak in intensity and narrow in bandwidth which restricts the application of these materials.

Fortunately, bismuth doped NIR luminescence materials exhibit super-broadband luminescence from 1000 to 1700 nm range covering all the fiber communication windows showing promising applications in broadband optical amplification and tunable fiber lasers. Recently, Bi-doped glass fibers and photonic crystal fibers have been fabricated,[2,11,12] and various types of fiber lasers have been demonstrated in the spectra region of 1140-1550 nm.[2] The maximal output power of Bi-doped fiber lasers achieved was above 20 W at 1460 nm[13] and the maximal power conversion efficiency has exceeded 60% at 1430 nm.[14] Moreover, efficient optical amplifiers in the 1240-1500 nm region with a maximum gain of over 20 dB and gain efficiency of 0.4 dB/mW at 1430 nm have also been developed.[2,14,15] When pumped by 780 or 808 nm, quantum efficiency of 1.0 ± 0.05 was obtained in Bi-doped AlGeP-silica fibers prepared by aerosol deposition.[16] On the other hand, optical waveguides have been fabricated in Bi-doped glasses.[17] Besides, NIR bioimaging has been performed in silica-coated bismuth-doped aluminosilicate nanoparticles.[18] In addition, due to the strong broad absorption in blue-green spectral range, high transmission at a wavelength larger than ~800 nm, and super-broadband NIR luminescence with high quantum efficiency, Bi-doped oxide glasses have been proposed as potential solar spectral converters and concentrators.[19]

Till now, NIR luminescence has been found in many kinds of materials.[20–48] However, the mechanism of NIR luminescence is still in controversy which restricts the development of various types of optical devices. Furthermore, the direct measurements of the valence state of bismuth ions with traditional instrumental approaches, e.g., electron energy loss spectroscopy (EELS), extended x-ray absorption fine structure (EXAFS) or X-ray photoelectron spectroscopy (XPS), may cause some artifacts since the valence state of bismuth species can be changed when irradiated with high energy beams such as electrons, X-ray, γ-ray, or fs laser.[20–25] Bi^{5+}, $Bi^{5+}O_n^{2-}$ or point defects was once proposed as the probable NIR active center;[26–28] however, they are contradict with other findings.[21,29–36,38] Much of current work put weight on bismuth with low valence states or bismuth cluster ions as the NIR active centers, such as Bi^{+},[20,37,49] Bi^0 interstitial atoms and other neutral bismuth clusters,[22,38] Bi_2^{4+},[32] Bi_2^{+},[47] Bi_2^{-},[40,50] Bi_2^{2-},[39,40,50,51] Bi_5^{3+} or Bi_8^{2+} cluster ions,[41,42] BiO or BiO_4 interstitial molecules,[30,52] complex formed by Bi^{+} or Bi^{2+} with certain anion vancanices, such as oxygen or fluorine vancanices.[43,53] Work of Hughes *et al.* on Bi-doped chalcogenide glass confirmed that BiO molecular is unlikely to be the NIR active center, since no oxygen exists in that glass.[39] Single bismuth center with four different types is proposed for NIR luminescence in Bi-doped aluminosilicate optical fibers.[54] Bi^{+} and Bi^0 together were ascibed to contribute to the NIR luminescence.[44] Recently, quantum chemical calculation has shown that none of the Bi^{+}, Bi_5^{3+}, and Bi_4^0 centers alone can give rise to the experimental NIR luminescence in Bi-doped solids; moreover, they revealed that Bi_5^{3+} cluster is not occurred in solid host other than zeolite due to its high electrical charge and high electron affinity.[55]

Though the NIR active centers are still not fully understood, most of the above mentioned bismuth species have their rationality as NIR active centers in the special materials. It is reasonable to envisage that several NIR active centers may coexist in the same material with one special bismuth species as the main NIR active center according to their chemical environment, and different materials may accomadate different active centers. If so, due to the different physical and chemical properties of these active centers, by modulating the concentration and chemical environment of these species, the emission wavelength and intensity could be tuned in a large scale. Moreover, if Bi neutral clusters or cluster ions can contribute to NIR luminescenece, bismuth concentration will have great effect on the NIR luminescecne properties of these species. Thus, controllable luminescence can be realized by many methods.

As GeO_2 can effectively promote the generation of NIR luminescent active centers, and sharply increases the luminescence intensity.[56] And the full width at half maximum (FWHM) of NIR luminescence in germanate glasses is ultrabroad.[57] Thus, we designed $MgO\text{-}Al_2O_3\text{-}GeO_2$ glass system as the host matrix. At present, tunable luminescence has been realized by many methods in rare-earth ions and transition metal ions doped materials; however, most of the methods were realized by changing ligang field in terms of modifying the host composition,[58] by controlling the energy transfer and luminescene intensity of several different dopants ions in terms of tailoring the distribution and concentration of these dopants ions.[59–61] Here, based on our supposition about the co-existence and different properties of several NIR bismuth active centers, we present three simple but efficient approaches to realize ultra-broadband controllable NIR luminescence covering 1000 to 1700 nm in the same glass host with only one dopant via modulating bismuth concentration, melting temperature, and atmosphere. It is found that the wavelength and intensity of NIR luminescence also depend greatly on the excitation wavelength. Excitingly, tunable red luminescence was observed and can also be tuned by the same methods. The chemical equilibrium of luminescence active centers is investigated systematically. The physical origin of the tunability and the near-infrared luminescence are discussed in depth. These results are hopeful to clarify the mechanism of NIR luminescence in Bi-doped materials and may potentially provide a scientific reference to realize controllable luminescence in materials doped with rare-earth and transition metal ions of multiple valence states. Our Bi-doped germanate glasses are multifunctional and show promise for applications in optical amplifiers, fiber lasers, photovoltaic energy conversion, light-emitting diodes (LEDs) and other fields.

II. EXPERIMENTAL PROCEDURE

Glass samples with the compositions of $20MgO\text{-}5Al_2O_3\text{-}75GeO_2\text{-}xBi_2O_3$ ($x = 0.1, 0.5, 1.0, 2.0, 4.0, 6.0$ in mol. %) were prepared by the melt-quenching method using analytical grade reagents MgO, Al_2O_3, GeO_2, and Bi_2O_3 as

raw materials. The 20 g batches corresponding to each composition were mixed homogeneously in agate mortar and then melted in a corundum crucible at 1500 °C for 30 min in air, Ar and 95%N_2/5%H_2 atmosphere, respectively. The 1.0 mol. % Bi-doped samples were also melted at 1400, 1450, 1550, and 1600 °C in air, respectively. The melts were cast into a slab on a stainless steel plate quickly and then annealed at 350 °C for 10 h to relieve the stress. The obtained glass samples were cut and polished into pieces with the size of $5 \times 5 \times 2$ mm^3.

The excitation (PLE), emission (PL) spectra and the fluorescence decay curves were measured using an FLS920 fluorescence spectrophotometer (Edinburgh Instrument Ltd., U.K.). The spectral resolution and time resolution are 1.0 nm and 1.0 μs, respectively. 450 W Xe lamp, 808 and 980 nm laser diodes are used as the exciting sources. Absorption spectra were recorded using UV3600 UV-Vis-NIR spectrophotometer (Shimadzu Corp., Japan). Electron spin resonance (ESR) spectra were measured using a ESRA-300 Electron Paramagnetic Resonance spectrometer (Bruker Corp., Germany) operating in the X-band frequency (= 9.8655 GHz) with the same amount of samples. All the measurements were taken at room temperature. The mean lifetime is calculated by the equation: $\tau_m = \int_{t_0}^{\infty} I(t)/I_{max} dt$, where $I(t)$ is the luminescence intensity at time t and $I_{max} = I(t_0)$ is the maximum of $I(t)$.

III. RESULTS AND DISCUSSION

If several NIR active centers coexist in the glasses, by controlling the relative amount of these centers and energy transfer among them, tunable luminescence can be realized. Inspired by this idea, we prepared Bi-doped glasses with different bismuth concentrations, melting temperatures, and atmospheres. NIR PL spectra of Bi-doped glasses with various bismuth concentrations at 1500 °C and 1.0 mol. % Bi-doped glass melted at different temperatures in air excited by 880 nm are shown in Figures 1(a) and 1(b), respectively. We confirmed that glass samples without Bi doping show no apparent visible and NIR emission. In Figure 1(a), only one peak at 1080 nm is observed for 0.1 mol. % Bi-doped glass. When the concentration is increased up to 0.5 mol. %, this peak red-shifts to 1090 nm and another peak at 1290 nm appears whose intensity is equal to that of the peak at 1090 nm; moreover, FWHM of the NIR PL is more than 500 nm showing overwhelming advantages than rare-earth-doped materials for optical communication. Due to the decrease of the detector sensitivity, the luminescent intensity falls sharply at around 1650 nm. As bismuth concentration increases to 1.0 mol. %, the emission peak has a red-shift to 1100 nm and a dominant peak at 1300 nm appears. With the further increase of bismuth concentration, the peak around 1100 nm diminishes at last, while the peak around 1300 nm red-shifts to 1375 nm and becomes the main peak. In Figure 1(b), when 1.0 mol. % Bi-doped glass is melted at temperatures from 1400 to 1600 °C in air, the emission wavelength and relative intensity can also been tuned. At 1400 °C, the emission intensity of the peaks around 1100 nm is a little stronger than that around 1300 nm. On the contrary, the intensity of the peak around 1300 nm grows stronger than that around 1100 nm at 1450 °C. Further rising the melting temperatures results in the dominant peak around 1300 nm and the increase of the intensity of both peaks reaching the maximum at 1550 °C. Then, the intensity of both peaks decreases at 1600 °C.

Not only bismuth concentration and melting temperature can lead to the tunable NIR PL, changing melting atmosphere can also result in the tunable luminescence. Figure 2 presents NIR PL spectra of 0.1, 0.5, and 1.0 mol. % Bi-doped glasses excited by 880 nm and melted in air, Ar, and 95%N_2/5%H_2 atmospheres, respectively. Compared with the 0.1 mol. % Bi-doped glass melted in air, when melted in Ar and 95%N_2/5%H_2, the intensity of the peak at around 1080 nm increases and a peak around 1300 nm appears and becomes dominant at last with a little red-shift of these peaks (Figure 2(a)). For the 0.5 mol. % Bi-doped glass melted in Ar, the peak around 1290 nm becomes dominant and both the peaks at 1090 and 1290 nm have a little red shift with the

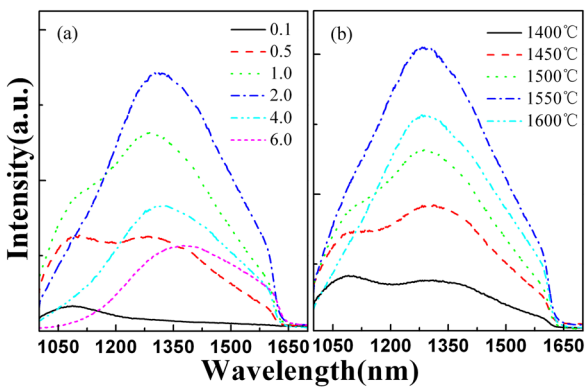

FIG. 1. (a) NIR PL spectra of Bi-doped glasses with various bismuth concentrations melted in air at 1500 °C, (b) NIR PL spectra of 1.0 mol. % Bi-doped glasses melted in air at various temperatures. All the spectra are excited by 880 nm.

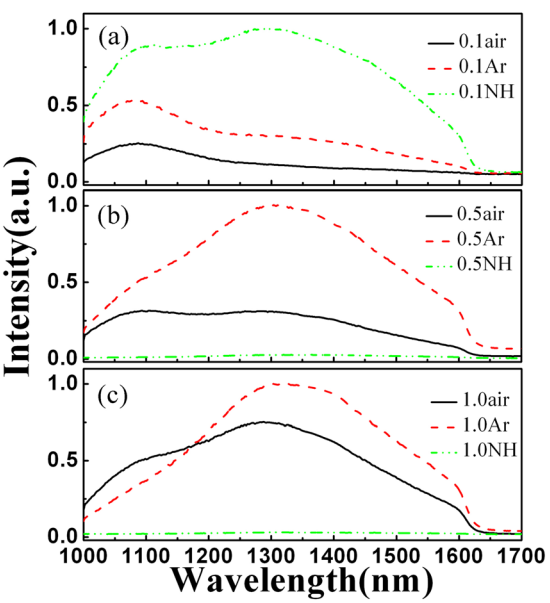

FIG. 2. NIR PL spectra of various concentrations of Bi-doped glasses prepared at 1500 °C in air, Ar and 95%N_2/5%H_2 (marked as NH) atmosphere, respectively: (a) 0.1 mol. %, (b) 0.5 mol. %, (c) 1.0 mol. %. All the spectra are excited by 880 nm.

increase of the intensity (Figure 2(b)). In Figure 2(c), when the glass is melted in Ar, the peak around 1100 nm nearly diminishes, while the peak around 1300 nm has a red-shift to 1330 nm and the intensity increases a little. Luminescence diminishes for both the 0.5 and 1.0 mol. % Bi-doped glasses melted in 95%N_2/5%H_2 atmosphere.

The tunable luminescence with the relative change of the two peaks at around 1100 and 1300 nm indicates that several NIR active centers coexist in the glasses. Appropriate increase of bismuth concentration and melting temperature is benefit for the generation of NIR active centers. And the decrease of the intensity of some peaks at high doping concentrations and melting temperatures may be caused by concentration quenching and energy transfer between different active centers. Su *et al*. found that 0.02 mol. % Bi-doped CsI single crystal only showed luminescence at around 1216 nm attributed to Bi^+ ions, while an additional emission band at 1560 nm originating from Bi_2^+ cluster ions could be observed in higher concentrations of Bi-doped CsI crystal.[47] It is rational to conclude that our concentration dependent luminescence here can also be related to bismuth clusters or cluster ions. Inert atmosphere is benefit for the generation of NIR active centers.[62] When the glasses are melted in Ar, more active centers will form in glasses leading to the increase of the intensity of the NIR emission. The decrease of the intensity of the peak at 1100 nm for the 1.0 mol. % Bi-doped glass melted in Ar atmosphere may be due to concentration quenching and energy transfer from the active centers related to the emission at 1100 nm to that around 1300 nm. The complete quenching of PL and absorption in the H_2-loaded and annealed SiAlGeP fibers have suggested that Bi metal atoms and/or Bi colloid or atomic clusters are not the NIR active centers.[63] However, the increase of the emission intensity for the 0.1 mol. % Bi-doped germanate glass melted in 95%N_2/5%H_2 atmosphere indicates that reducing atmosphere is benefit for the NIR luminescence when bismuth concentration is low and Bi metal atoms and atomic clusters may contribute to the NIR PL. The relative increase of the weight of the luminescence at around 1300 nm in contrast with that at around 1080 nm for the 0.1 mol. % Bi-doped germanate glass melted in 95%N_2/5%H_2 atmosphere further confirms that luminescence at around 1300 nm comes from bismuth species with lower valence state than that at 1100 nm. For the 0.5 and 1.0 mol. % Bi-doped glass melted in 95%N_2/5%H_2 atmosphere, the color of the glasses has become completely black, so the diminish of the luminescence may be due to the absorption and scattering of the formed Bi colloid. The changes of Bi species in glasses melted in 95%N_2/5%H_2 atmosphere can be expressed as follows:

$$Bi^{3+} \rightarrow Bi^{2+} \rightarrow Bi^{+} \rightarrow Bi^{0}, \text{Bi clusters and cluster ions} \rightarrow \text{Bi colloid}. \quad (1)$$

In order to reveal the origin of the tunable luminescence in the glasses, absorption spectra of glasses with different bismuth concentration melted in air at 1500 °C are shown in Figure 3. Two apparent absorption bands at around 520 and

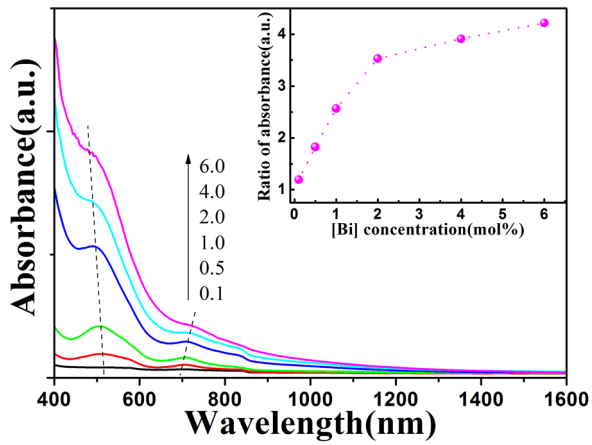

FIG. 3. Absorption spectra of Bi-doped glasses melted in air at 1500 °C with various bismuth concentrations (the concentration is 0.1, 0.5, 1.0, 2.0, 4.0, and 6.0 mol. %, respectively). The inset is the ratio of the absorbance of the band at around 520 nm to that at 700 nm as a function of bismuth concentration.

700 nm are observed. The band at around 830 nm is caused by the change of grating slit. As bismuth concentration increases, the peak at 520 nm blue-shifts to 485 nm, while the band at 700 nm shifts towards the reverse direction to 720 nm. The inset shows the ratio of the absorbance of the bands at around 520 nm to that at 700 nm. With the increase of bismuth concentration, the ratio rises from about 1.0 to above 4.0. The absorption band at around 485 nm becomes dominant at last. The different increase extent of the two bands indicates that these two bands correlate to two different active centers. The reverse shifting directions of the two bands imply that there are other active centers in the glasses besides the two active centers. Thus, there are at least three active centers in the glasses. The absorption bands of glasses melted in different atmospheres and temperatures also show the same changing trend (Supplementary material, Fig. S1).[69] When melted in 95%N_2/5%H_2 atmosphere, 0.1 mol. % Bi-doped glass has strong absorption bands at 490 and 710 nm. While for 0.5 mol. % Bi-doped glass, only an absorption band at around 710 nm can be observed, the large red-shift of the absorption edge may be due to the scattering of Bi colloid for the glass is nearly black.[64] For 1.0 mol. % Bi-doped glass, it is completely black and no absorption bands of Bi NIR active centers can be observed due to the strong scattering of Bi colloid. Thus, the utilizing of reducing atmosphere benefits to the generation of NIR active centers when bismuth concentration is low.

In addition, the Gaussian fitting results of the tunable luminescence demonstrate that when 0.1 mol. % Bi-doped glass melted in air at 1500 °C is excited by 808 and 980 nm, only one peak occurs at 1250 (8000 cm^{-1}) and 1100 nm (9090 cm^{-1}), respectively (Supplementary material, Figs. S2(b) and S3(b)).[69] While for higher doping concentration, such as 2.0 mol. %, two Gaussian fitting peaks located at 1260 (7937 cm^{-1}) and 1440 nm (6944 cm^{-1}) are observed when the glass is excited by 808 nm (Supplementary material, Fig. S2(c))[69] and three Gaussian fitting peaks appear at 1117 (8950 cm^{-1}), 1260 and 1450 nm (6897 cm^{-1}) when it is excited by 980 nm, respectively (Supplementary material,

Fig. S3(c)).[69] Moreover, with the increase of bismuth concentration, the ratio of the intensity of the emission at 1260 and 1450 nm to that at 1100 nm rises and reaches above 1.0 at last (Supplementary material, the inset of Fig. S3(a))[69] indicating that emission at around these wavelengths originates from different active centers and there may be three NIR active centers in the glasses. Here, we named the active centers contributing to the luminescence around 1100, 1260, and 1450 nm as NIRA, NIRB, and NIRC, respectively. Similar results have been found by Hughes *et al.* in Bi-doped lead-germanate glasses that when excited by 974 nm, two Gaussian fitting peaks at 1090 and 1330 nm were observed in the 0% PbO content glass, while two peaks centered at 1110 and 1475 nm appeared in the 22% PbO content glass, and only one peak was found at 1000 nm in the 24% PbO content glass.[65]

PLE spectra of 1.0 mol. % Bi-doped glass melted in air at 1500 °C and monitored at 1080, 1260, and 1450 nm are presented in Figure 4(a). For the emission at 1080 nm, excitation bands are observed at 335, 535, and 702 nm with a shoulder around 480 nm. Excitation bands locating at 350, 480, and 730 nm together with a shoulder around 520 nm are observed when monitored at 1260 nm. For the emission at 1450 nm, excitation band at 480 nm and three weak shoulders at 380, 520, and 800 nm can be observed. The sharp peaks at 466, 823, and 880 nm are caused by xenon lamp. The different excitation spectra further indicate that three active centers coexist in the glasses. Thus by tuning excitation wavelength, emission wavelength can be tuned in a large scale.

We performed the excitation wavelength dependent emission peak position change of 1.0 mol. % Bi-doped glass in the inset of Figure 4(a). The emission peak shows a red-shift from 1134 to 1220 nm when the excitation wavelength changes from 300 to 420 nm. As the excitation wavelength increases from 440 to 580 nm, the emission peak blue-shifts from 1213 to 1106 nm. Interestingly, the emission peak shows a slight red-shift from 1112 to 1180 nm when changing the excitation wavelength from 600 to 620 nm. Further increase the excitation wavelength from 640 to 680 nm results in the blue-shift of the emission peak from 1146 to 1080 nm, again. When the excitation wavelength is increased from 700 to 900 nm, the emission peak shows a red-shift from 1102 to 1330 nm. Finally, the emission peak shows a blue shift to 1125 nm while excited at 980 nm. The shift of the peak position is due to the overlap of the luminescence from different active centers (Supplementary material, Fig. S4).[69] The fluorescent decay curves of 1.0 mol. % Bi-doped glass are shown in Figure 4(b). All curves show second-order exponential decay. The shorter lifetime for the emission at 1080, 1260, and 1450 nm is 129.5, 167.2, and 80.3 μs, respectively, while the longer lifetime for the emission at 1080, 1260, and 1450 nm is 408.8, 514.5, and 311.8 μs, respectively. The calculated lifetime of the emission at 1080, 1260, and 1450 nm is 273.3, 327.4, and 170.7 μs, respectively. Due to the lower pumping power density of the excitation sources, no photo-darkening effect has been observed in our experiments. Thus, the second-order exponential decay and the different lifetime may originate from the co-existence of several NIR active centers rather than the effect of photo-darkening.

To further reveal which bismuth species contribute to the respective emission, ESR spectra of undoped, 0.1 and 1.0 mol. % Bi-doped glasses are presented in Figure 5. In Bi-doped NIR emission zinc aluminosilicate glasses and glass ceramics, ESR signal originating from Bi_2^- was found at g $\approx$ 2.20.[10] However, no signal at around g $\approx$ 2.20 is observed in Figure 5 indicating that Bi_2^- does not exist in our glasses. As there is no signal at g = 2.0086, Bi_2^+ can also be excluded in our glasses.[47] The undoped glass shows a signal at g = 1.993. This signal is attributed to GeO_4^- trapped-electron centers which comes from electrons trapped on the GeO_4^0 units.[66] This signal weakens for 0.1 mol. % Bi-doped glass, and it diminishes for 1.0 mol. % Bi-doped glass. Fujimoto and Nakatsuka carried out the ESR spectra of Bi-doped silica glasses with high bismuth concentration, no ESR signal was detected, thus they concluded that the NIR active centers were Bi^{5+}.[26] However, the ESR spectra of bismuth un-doped glasses were not yet examined and the possible active centers such as Bi^+ and Bi_2^{2-} are ESR-inactive. The weakening and

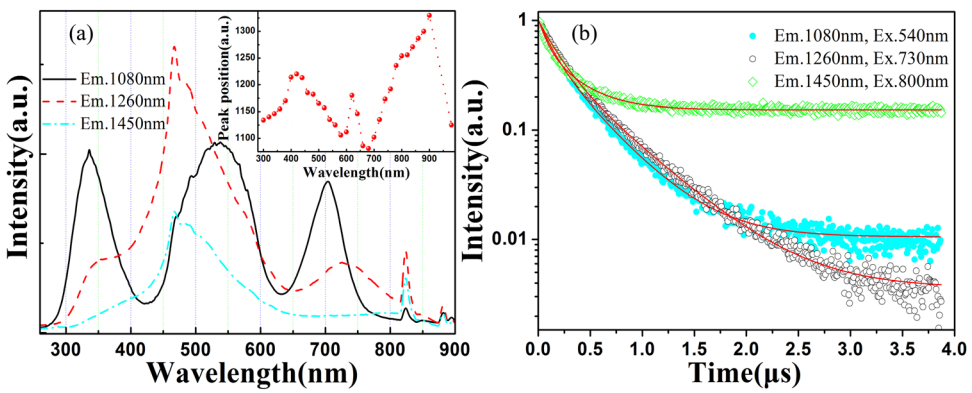

FIG. 4. (a) PLE spectra of 1.0 mol. % Bi-doped glass melted in air at 1500 °C and monitored at 1080, 1260, and 1450 nm, respectively. The inset is the dependence of emission wavelengths on excitation wavelengths from 300 to 980 nm. (b) Fluorescence decay curves of 1.0 mol. % Bi-doped glass melted in air at 1500 °C. The excitation wavelengths are 540, 730, and 800 nm, and the corresponding emission wavelengths are 1080, 1260, and 1450 nm, respectively. The correlated coefficients for the fits by bi-expotential decay equation for this emission (1080 nm: $I = 0.51952\,e^{-t/408.8} + 0.47049\,e^{-t/129.5}$, 1260 nm: $I = 0.54531\,e^{-t/167.2} + 0.45922\,e^{-t/514.5}$, 1450 nm: $I = 0.43735\,e^{-t/311.8} + 0.43972\,e^{-t/80.3}$) are 0.9992, 0.9995, and 0.9958, respectively.

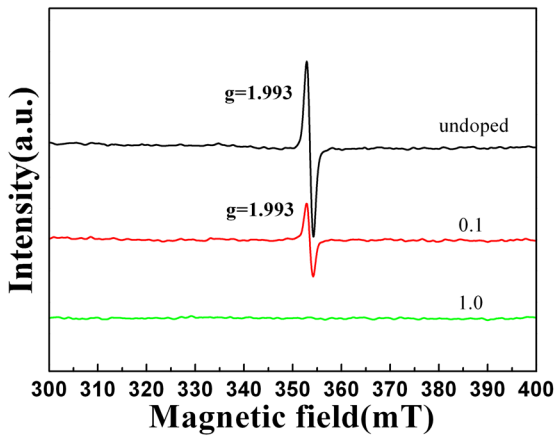

FIG. 5. ESR spectra of undoped, 0.1 and 1.0 mol. % Bi-doped glasses melted in air at 1500 °C.

disappearance of the signal with the increase of bismuth concentration indicate that the trapped-electron centers in glasses combine with Bi ions of high valence state forming Bi ions of lower valence state. Moreover, the increase of the luminescence in reducing atmosphere in our experiments confirms that the NIR active centers are bismuth species with low valence states. Based on the analysis of high-resolution synchrotron powder X-ray diffraction data, direct experimental evidence of the formation of monovalent Bi (i.e., Bi^{+}) was observed in NIR luminescent zeolite Y.[49] In Bi-doped $M_2P_2P_7$ (M = Ca, Sr, Ba) crystals prepared in CO atmosphere, NIR luminescence could only be detected in Bi-doped $Ba_2P_2O_7$ crystal, based on the radius and charge mismatch between the cation site and the bismuth species, Peng *et al.* proposed that Bi^{0} contributed to the NIR luminescence.[46] Hughes *et al.*[39] observed NIR emission from Bi-doped chalcogenide glasses based on Bi_2^{2-} which had emission bands around 1500 nm. Recently, Sun *et al.* found NIR luminescence in Bi-doped $(K\text{-crypt})_2Bi_2$ single crystal originating from the inherent electronic transition of Bi_2^{2-}.[51] However, none of these active center alone can explain the tunable luminescence here. Based on the excitation wavelength dependent emission wavelength change, excitation spectra, lifetime as well as the luminescence properties after heat-treatment, Zhang *et al.* proposed that the origin of the luminescence around 1100 and 1260 nm can be ascribed to Bi^{+} and Bi^{0}, respectively.[44] But they neglected the luminescence properties excited by the wavelengths longer than 850 nm and no shoulders around 1450 nm were found in their luminescence spectra. As discussed above, the luminescence at higher bismuth concentration may be related to bismuth clusters or cluster ions. And luminescence at longer wavelength comes from bismuth species with lower valence states than that at shorter wavelength. Thus, based on our results, Bi^{+} and Bi^{0} are probably contribute to the luminescence at around 1100 and 1260 nm, respectively. And bismuth clusters or cluster ions, e.g., Bi_2^{2-}, may correspond to the emission band at around 1450 nm. The ultra-broadband tunable luminescence covering 1000 to 1700 nm range with broad excitation bands across the visible light range makes Bi-doped glasses as multifunctional materials for potential applications in optical devices.

Red visible luminescence of Bi-doped glasses melted in air at 1500 °C with different bismuth concentrations excited by 395 and 450 nm is shown in Figures 6(a) and 6(b), respectively. When excited by 395 nm, the emission peak locates at 720 nm and its intensity decreases as bismuth concentration increases. When excited by 450 nm, only one peak at 720 nm is observed at the bismuth concentration of 0.1 mol. %. Further increase the concentration results in the decrease of the intensity of the peak at 720 nm. And another dominant peak

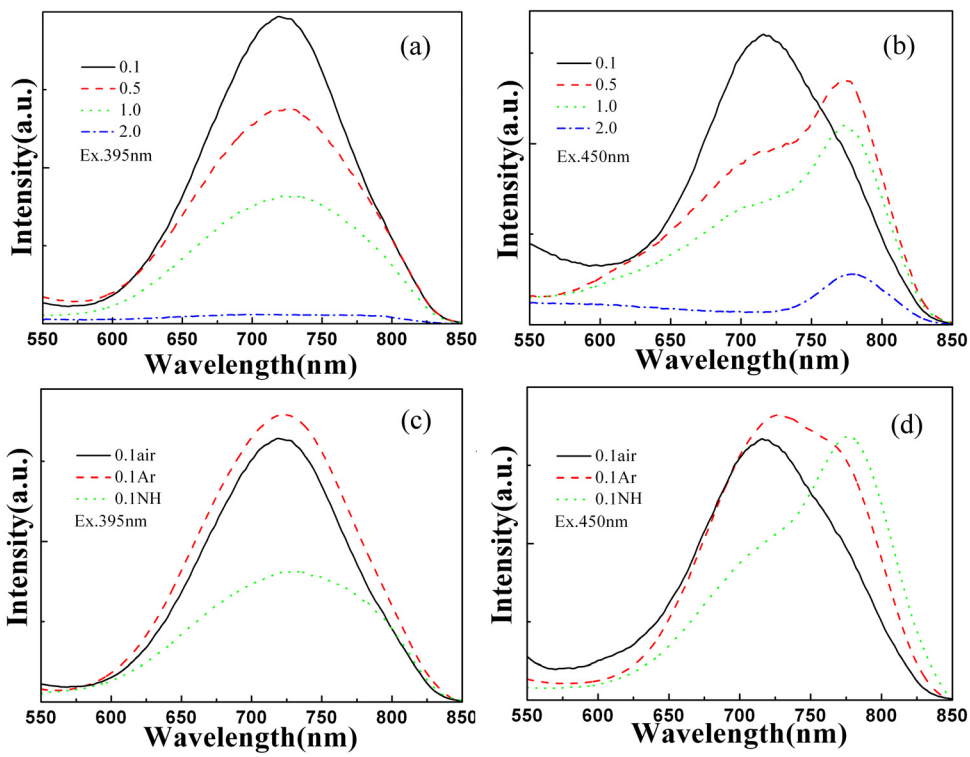

FIG. 6. (a) and (b) Visible luminescence spectra of Bi-doped glasses melted in air at 1500 °C with various bismuth concentrations (0.1, 0.5, 1.0, and 2.0 mol. %) excited by 395 and 450 nm, respectively. (c) and (d) Visible luminescence spectra of 0.1 mol. % Bi-doped glasses melted in air, Ar and $95\%N_2/5\%H_2$ atmosphere at 1500 °C, respectively. The excitation wavelengths are 395 and 450 nm, respectively.

at 780 nm occurs whose intensity reaches the maximum at the concentration of 0.5 mol. %. The emission intensity at 780 nm for 0.5 and 1.0 mol. % Bi-doped glasses is stronger than that of 0.1 mol. % Bi-doped glass. Only one peak at 780 nm occurs when bismuth concentration is 2.0 mol. %. Figures 6(c) and 6(d) present visible luminescence spectra of 0.1 mol. % Bi-doped glasses melted in air, Ar and 95%N_2/5%H_2 atmospheres excited by 395 and 450 nm, respectively. When excited by 395 nm, the emission intensity of the peak at 720 nm for the glasses melted in Ar and 95%N_2/5%H_2 atmosphere is stronger and weaker than that melted in air, respectively. On the other hand, compared with the glass melted in air, when melted in Ar and excited by 450 nm, the intensity of the peak at 720 nm increases and another peak at 780 nm appears. For the glass melted in 95%N_2/5%H_2, the intensity of the peak at 720 nm decreases to the lowest, while the peak at 780 nm is dominant and its intensity is stronger than that melted in air and Ar. For the 1.0 mol. % Bi-doped glasses melted in air, three broad excitation bands at 310, 395, and 615 nm are observed when monitored at 720 nm, while monitored at 780 nm, excitation bands locate at 320, 450, and 625 nm, respectively (Supplementary material, Fig. S5).[69] Bi^{2+} has characteristic red luminescence and three excitation bands.[67] By changing doping concentration of Bi-doped $Sr_2P_2O_7$ crystal, two red emission bands ascribed to Bi^{2+} in two Sr sites are observed when excited by 450 nm.[68] For germanate glasses, the two bands at 720 and 780 nm of our results may also come from Bi^{2+} in two distinct sites and their relative content can be controlled to realize wavelength and intensity tunable luminescence via changing excitation wavelength, doping level, and melting atmosphere. Due to the superbroad excitation bands covering from the UV to orange red color range, and tunable red emission, Bi-doped germanate glasses have potential applications as red luminescence materials for UV and Blue LEDs.

IV. CONCLUSION

In summary, ultra-broadband NIR luminescence from 1000 to 1700 nm with the largest FWHM of about 500 nm covering the whole windows of optical communication is observed in bismuth-doped germanate glasses. Three facile and effective approaches are presented in order to realize tunable luminescence in the same host material with only one kind of dopant—modulating bismuth concentration, melting temperature and atmosphere. Emission wavelength is also tunable when excited by light with the wavelength from 300 to 980 nm. We found that the emission intensity is enhanced when increasing preparation temperatures from 1400 to 1550 °C and melting glass with low doping level in inertia or reducing atmosphere. With the increase of bismuth concentration, the different increase extent and reverse shifting directions of the two absorption bands at around 520 and 700 nm rises indicate that near-infrared luminescence originates from at least three bismuth species with low valence states and luminescence at longer wavelength comes from bismuth species with lower valence states than that at shorter wavelength. With the increase of melting temperatures and the increase of reducing extent of the preparation atmosphere, bismuth species transform from Bi^{3+} to Bi^{2+}, Bi^{+}, Bi^{0} and bismuth clusters, and then to bismuth colloid. Three bismuth active centers, namely Bi^{+} ions, Bi^{0} atoms, and Bi cluster ions, such as Bi_2^{2-} dimer ions, were proposed as the probable active centers for the NIR luminescence at around 1100, 1260, and 1450 nm, respectively. GeO_4^{-} trapped-electron centers can react with bismuth species of high valence state to form bismuth near-infrared active centers of low valence state. The result deepens our understanding of the interaction of defects in glasses with dopant. Doping concentration, energy transfer, and chemical equilibrium of different bismuth active centers can be tailored with the advantage of displaying dual-modulating mode of luminescence. Red luminescence with two peaks at 720 and 780 nm originating from Bi^{2+} ions in two distinct sites is also found, which can be tuned by modulating bismuth concentration, melting atmosphere, and excitation wavelength. These strategies of realizing tunable luminescence in the same host with only one kind of dopant can also be applied in materials doped with rare-earth and transition metal ions of multiple valence states. These dual-modulating modes of red visible and ultra-broadband near-infrared luminescence materials with broad absorption in soft ultraviolet to orange red range and super-broad excitation bands have special advantages for multifunctional tunable light sources with various applications from light-emitting diodes, optical fiber communication to photovoltaic energy conversion.

ACKNOWLEDGMENTS

This work was financially supported by the National Natural Science Foundation of China (Grant Nos. 51072054, 51132004, and 51102209), National Basic Research Program of China (2011CB808100), the Fundamental Research Funds for the Central Universities, and the Open Fund of the State Key Laboratory of Modern Optical Instrumentation (Zhejiang University). This work was also supported by the Hong Kong Polytechnic University Joint Ph.D. Supervision Scheme (A-SA77).

[1]S. V. Eliseevaa and J. G. Bünzli, Chem. Soc. Rev. **39**, 189 (2010).
[2]E. M. Dianov, Light: Science & Applications **1**, e12 (2012).
[3]A. Luque, J. Appl. Phys. **110**, 031301 (2011).
[4]M. G. Debije and P. P. C. Verbunt, Adv. Energy Mater. **2**, 12 (2012).
[5]R. Dewan, I. Vasilev, V. Jovanov, and D. Knipp, J. Appl. Phys. **110**, 013101 (2011).
[6]S. Fischer, J. C. Goldschmidt, P. Löper, G. H. Bauer, R. Brüggemann, K. Krämer, D. Biner, M. Hermle, and S. W. Glunz, J. Appl. Phys. **108**, 044912 (2010).
[7]K. Taira and J. Nakata, Nat. Photonics **4**, 602 (2010).
[8]A. Deinega and S. John, J. Appl. Phys. **112**, 074327 (2012).
[9]K. X. Wang, Z. Yu, V. Liu, Y. Cui, and S. Fan, Nano Lett. **12**, 1616 (2012).
[10]Q. Duan, F. Qin, D. Wang, W. Xu, J. Cheng, Z. Zhang, and W. Cao, J. Appl. Phys. **110**, 113503 (2011).
[11]I. A. Bufetov and E. M. Dianov, Laser Phys. Lett. **6**, 487 (2009).
[12]I. Razdobreev, H. E. Hamzaoui, L. Bigot, V. Arion, G. Bouwmans, A. L. Rouge, and M. Bouazaoui, Opt. Express **18**, 19479 (2010).
[13]A. Shubin, I. Bufetov, M. Melkumov, S. Firstov, O. Medvedkov, V. Khopin, A. Guryanov, and E. Dianov, Opt. Lett. **37**, 2589 (2012).
[14]M. A. Melkumov, I. A. Bufetov, A. V. Shubin, S. V. Firstov, V. F. Khopin, A. N. Guryanov, and E. M. Dianov, Opt. Lett. **36**, 2408 (2011).
[15]I. Bufetov, S. Firstov, V. Khopin, O. Medvedkov, A. Guryanov, and E. Dianov, Opt. Lett. **33**, 2227 (2008).

[16]R. S. Quimby, R. L. Shubochkin, and T. F. Morse, Opt. Lett. **34**, 3181 (2009).
[17]B. Zhou, H. Lin, B. Chen, and E. Y. B. Pun, Opt. Express **19**, 6514 (2011).
[18]H. Sun, J. Yang, M. Fujii, Y. Sakka, Y. Zhu, T. Asahara, N. Shirahata, M. Ii, Z. Bai, J. Li, and H. Gao, Small **7**, 199 (2011).
[19]M. Peng and L. Wondraczek, J. Mater. Chem. **19**, 627 (2009).
[20]B. Xu, S. Zhou, M. Guan, D. Tan, Y. Teng, J. Zhou, Z. Ma, Z. Hong, and J. Qiu, Opt. Express **19**, 23436 (2011).
[21]J. Xu, H. Zhao, L. Su, J. Yu, P. Zhou, H. Tang, L. Zheng, and H. Li, Opt. Express **18**, 3385 (2010).
[22]M. Peng, J. Qiu, D. Chen, X. Meng, and C. Zhu, Opt. Lett. **30**, 2433 (2005).
[23]S. Zhou, W. Lei, N. Jiang, J. Hao, E. Wu, H. Zeng, and J. Qiu, J. Mater. Chem. **19**, 4603 (2009).
[24]Y. Fujimoto, J. Am. Ceram. Soc. **93**, 581 (2010).
[25]M. Peng, G. Dong, L. Wondraczek, L. Zhang, N. Zhang, and J. Qiu, J. Non-Cryst. Solids **357**, 2241 (2011).
[26]Y. Fujimoto and M. Nakatsuka, Jpn. J. Appl. Phys., Part 2 **40**, L279 (2001).
[27]I. Razdobreev, V. Y. Ivanov, L. Bigot, M. Godlewski, and E. F. Kustov, Opt. Lett. **34**, 2691 (2009).
[28]M. Y. Sharonov, A. B. Bykov, V. Petricevic, and R. R. Alfano, Opt. Lett. **33**, 2131 (2008).
[29]X. Meng, J. Qiu, M. Peng, D. Chen, Q. Zhao, X. Jiang, and C. Zhu, Opt. Express **13**, 1628 (2005).
[30]J. Ren, L. Yang, J. Qiu, D. Chen, X. Jiang, and C. Zhu, Solid State Commun.**140**, 38 (2006).
[31]B. Xu, D. Tan, M. Guan, Y. Teng, J. Zhou, J. Qiu, and Z. Hong, J. Electrochem. Soc. **158**, G203 (2011).
[32]A. N. Romanov, Z. T. Fattakhova, A. A. Veber, O. V. Usovich, E. V. Haula, V. N. Korchak, V. B. Tsvetkov, L. A. Trusov, P. E. Kazin, and V. B. Sulimov, Opt. Express **20**, 7212 (2012).
[33]H. Sun, A. Hosokawa, Y. Miwa, F. Shimaoka, M. Fujii, M. Mizuhata, S. Hayashi, and S. Deki, Adv. Mater. **21**, 3694 (2009).
[34]L. Su, P. Zhou, J. Yu, H. Li, L. Zheng, F. Wu, Y. Yang, Q. Yang, and J. Xu, Opt. Express **17**, 13554 (2009).
[35]H. Masai, Y. Takahashi, T. Fujiwara, T. Suzuki, and Y. Ohishi, J. Appl. Phys. **106**, 103523 (2009).
[36]Y. Arai, T. Suzuki, Y. Ohishi, S. Morimoto, and S. Khonthon, Appl. Phys. Lett. **90**, 261110 (2007).
[37]S. Zhou, N. Jiang, B. Zhu, H. Yang, S. Ye, G. Lakshminarayana, J. Hao, and J. Qiu, Adv. Funct. Mater. **18**, 1407 (2008).
[38]M. Peng, C. Zollfrank, and L. Wondraczek, J. Phys.: Condens. Matter **21**, 285106 (2009).
[39]M. A. Hughes, T. Akada, T. Suzuki, Y. Ohishi, and D. W. Hewak, Opt. Express **17**, 19345 (2009).
[40]S. Khonthon, S. Morimoto, Y. Arai, and Y. Ohishi, J. Ceram. Soc. Jpn. **115**, 259 (2007).
[41]H. Sun, Y. Sakka, H. Gao, Y. Miwa, M. Fujii, N. Shirahata, Z. Bai, and J. Li, J. Mater. Chem. **21**, 4060 (2011).
[42]H. Sun, Y. Sakka, N. Shirahata, H. Gao, and T. Yonezawa, J. Mater. Chem. **22**, 12837 (2012).
[43]J. Ruan, L. Su, J. Qiu, D. Chen, and J. Xu, Opt. Express **17**, 5163 (2009).
[44]N. Zhang, J. Qiu, G. Dong, Z. Yang, Q. Zhang, and M. Peng, J. Mater. Chem. **22**, 3154 (2012).
[45]A. G. Okhrimchuk, L. N. Butvina, E. M. Dianov, N. V. Lichkova, V. N. Zagorodnev, and K. N. Boldyrev, Opt. Lett. **33**, 2182 (2008).
[46]M. Peng, B. Sprenger, M. A. Schmidt, H. G. L. Schwefel, and L. Wondraczek, Opt. Express **18**, 12852 (2010).
[47]L. Su, H. Zhao, H. Li, L. Zheng, X. Fan, X. Jiang, H. Tang, G. Ren, J. Xu, W. Ryba-Romanowski, R. Lisiecki, and P. Solarz, Opt. Mater. Express **2**, 757 (2012).
[48]H. Sun, Y. Sakka, M. Fujii, N. Shirahata, and H. Gao, Opt. Lett. **36**, 100 (2011).
[49]H. Sun, Y. Matsushita, Y. Sakka, N. Shirahata, M. Tanaka, Y. Katsuya, H. Gao, and K. Kobayashi, J. Am. Chem. Soc. **134**, 2918 (2012).
[50]V. O. Sokolov, V. G. Plotnichenko, and E. M. Dianov, Opt. Lett. **33**, 1488 (2008).
[51]H. Sun, T. Yonezawa, M. Gillett-Kunnath, Y. Sakka, N. Shirahata, M. Fujii, and S. Sevov, J. Mater. Chem. **22**, 20175 (2012).
[52]E. F. Kustov, L. I. Bulatov, V. V. Dvoyrin, and V. M. Mashinsky, Opt. Lett. **34**, 1549 (2009).
[53]E. M. Dianov, Quantum Electron. **40**, 283 (2010).
[54]L. I. Bulatov, V. M. Mashinsky, V. V. Dvoyrin, E. F. Kustov, and E. M. Dianov, Quantum Electron. **40**, 153 (2010).
[55]V. O. Sokolov, V. G. Plotnichenko, and E. M. Dianov, e-print arXiv:1106.1519v2 condmat.mtrl-sci (2011).
[56]Y. Fujimoto, Y. Hirata, Y. Kuwada, T. Sato, and M. Nakatsuka, J. Mater. Res. **22**, 565 (2007).
[57]J. Ren, J. Qiu, B. Wu, and D. Chen, J. Mater. Res. **22**, 1574 (2007).
[58]S. Zhou, N. Jiang, B. Wu, J. Hao, and J. Qiu, Adv. Funct. Mater. **19**, 2081 (2009).
[59]S. Zhou, N. Jiang, K. Miura, S. Tanabe, M. Shimizu, M. Sakakura, Y. Shimotsuma, M. Nishi, J. Qiu, and K. Hirao, J. Am. Chem. Soc. **132**, 17945 (2010).
[60]J. Yang, C. Zhang, C. Peng, C. Li, L. Wang, R. Chai, and J. Lin, Chem. Eur. J. **15**, 4649 (2009).
[61]F. Wang, R. Deng, J. Wang, Q. Wang, Y. Han, H. Zhu, X. Chen, and X. Liu, Nature Mater. **10**, 968 (2011).
[62]X. Jiang and A. Jha, Opt. Mater. **33**, 14 (2010).
[63]V. G. Truong, L. Bigot, A. Lerouge, M. Douay, and I. Razdobreev, Appl. Phys. Lett. **92**, 041908 (2008).
[64]G. Lin, D. Tan, F. Luo, D. Chen, Q. Zhao, and J. Qiu, J. Non-Cryst. Solids **357**, 2312 (2011).
[65]M. Hughes, T. Suzuki, and Y. Ohishi, J. Opt. Soc. Am. B **25**, 1380 (2008).
[66]D. L. Griscom, J. Non-Cryst. Solids **357**, 1945 (2011).
[67]G. Blasse, A. Meijerink, M. Nomes, and J. Zuidema, J. Phys. Chem. Solids **55**, 171 (1994).
[68]M. Peng and L. Wondraczek, Opt. Lett. **35**, 2544 (2010).
[69]See supplementary material at http://dx.doi.org/10.1063/1.4791698 for Absorption spectra, NIR PL spectra, visible PLE spectra and dependence of relative NIR emission intensity and FWHM on excitation wavelengths of Bi-doped glass.